Line Profiles of Ni-like Collisional XUV Laser Amplifiers: Particle Correlation Effects

Annette Calisti, Sandrine Ferri, Caroline Mossé, Bernard Talin, Annie Klisnick, Limin Meng, Djamel Benredjem, Olivier Guilbaud

Line Profiles of Ni-like Collisional XUV Laser Amplifiers: Particle Correlation Effects

A. Calisti,* S. Ferri, C. Mossé, and B. Talin
Aix-Marseille Université, CNRS, PIIM UMR7345,
centre Saint Jérôme, case 232, 13397 Marseille Cedex 20, France.

A. Klisnick and L. Meng
ISMO, UMR8214, Université Paris-Sud 11 - CNRS,
Bat. 350, 91405 Orsay Cedex, France.

D. Benredjem
LAC, UPR3321, CNRS, Université Paris-sud 11, 91405 Orsay, France.

O. Guilbaud
LPGP, UMR8578, CNRS - Université Paris-Sud 11, Bat. 210, 91405 Orsay Cedex, France.
(Dated: July 23, 2012)

The effects of particle correlations on the spectral broadening due to the radiator motion (Doppler broadening) are discussed for a Ni-like XUV laser line pumped in two different regimes of collisional excitation. The transient pumping for which ionic temperature is relatively low (the plasma coupling parameters is large), and the quasi steady-state pumping (QSS) for which the ionic temperature is higher and the plasma coupling parameter of the order of 1 are considered. It is shown by using classical Molecular Dynamics simulation techniques that in both cases the effect of correlations modify the radiator-motion broadened profiles and cannot be neglected in evaluating Doppler effect. This is due to the fact that the radiator velocity changes during the radiation emission resulting in a mixing of velocities in the line profile. It is also shown that this results in a homogenization of the intrinsic line profiles.

PACS numbers: 32.70.Jz, 42.55.Vc, 52.20.-j, 52.25.-b, 52.65.Yy

* annette.calisti@univ-amu.fr

I. INTRODUCTION

The intrinsic (optically thin) spectral profile of emission lines in a plasma is determined predominantly by spontaneous emission rates, electron collisional rates, Stark broadening and Doppler broadening [1] with possible complications due to ion turbulence [2] and additional ion-ion interactions [2–5]. In medium with population inversions and gain, the observed profile is modified by radiative transport effects in being narrowed approximatively as the square root of the gain-length product in the small signal regime [6]. As the laser saturates, if the intrinsic profile is dominated by inhomogeneous rather than homogeneous broadening mechanisms, the line can be re-broadened to its intrinsic width. This points out clearly the importance of having a good representation of the intrinsic profile together with a good understanding of the different mechanisms responsible for broadening. It is usual to consider that the inhomogeneous broadening mechanisms are caused by the local inhomogeneities of the medium such as Doppler shifts, quasi-static electric microfields or turbulence and that homogeneous broadenings are mainly due to electron-radiator collisions and/or spontaneous emission. Nevertheless, similarly to the quasi-static electric field approximation which can be inappropriate in the Stark broadening theory due to perturber ion dynamics [7], the free particle formalism involved in the standard Doppler effect calculation could fail if ion velocities change over time scales of the same order of or shorter than the effective radiative lifetime of the oscillator (i.e. the inverse of homogeneous spectral linewidth). In other words, if the velocities change before the light emission happens, it is no longer possible to consider ions with straight trajectories and a calculation, taking into account particle interactions, has to be done. In some circumstances, the breakdown of the free particle approximation can result in the effective "homogenization" of the ordinarily inhomogeneous Doppler profile by velocity redistribution when the mean time of velocity-changing, t_c, is less than the effective radiative lifetime or in the narrowing of the Doppler profile when t_c is shorter than the effective Doppler correlation time (Dicke narrowing [8]).
In this work, a detailed analysis of the different broadening mechanisms of the spectral profiles of the $4d - 4p$ ($J = 0 - 1$) lasing line in Ni-like Ag ($\lambda = 13.9$ nm) is performed. The plasma temperatures and densities that are consistent with the ones required for collisional excitation pumping of Ni-like Ag in laser-produced plasmas, give rise to a strong coupling plasma regime where correlations between particles can no longer be ignored. A study on the accuracy of the free-particle Doppler approximation, versus density and temperature has been done by using classical molecular dynamics (MD) simulations, for the Ni-like Ag lasing line and for conditions relevant for both transient and quasi-steady state (QSS) pumping regimes. It is shown that even though important differences of behavior of the intrinsic line profiles between these two laser regimes appear, the effects of particle interactions on the Doppler profiles are not negligible and can be modelled in a good approximation in the same manner.

II. SPECTRAL LINE SHAPE MODELING

The general expression of the line profile is given by the Fourier-transform of the correlation function, $C(t)$, of the radiator dipole operator, $\mathbf{d}$:

$$I(\omega) = \Re e \frac{1}{\pi} \int_0^\infty dt C(t) e^{i\omega t} \tag{1}$$

with,

$$C(t) = \ll \mathbf{d}^\dagger | \{U_l(t)\}_{\text{bath}} | \mathbf{d}\rho_0 \gg \tag{2}$$

in the Liouville space.

Here, ρ_0 is the equilibrium density matrix and $\{U_l(t)\}_{\rm bath}$ is the bath-averaged evolution operator of the emitter. $U_l(t)$ is solution of the following stochastic Liouville equation (SLE) :

$$\frac{dU_l(t)}{dt} = -iL_l.U_l(t) \tag{3}$$

with the condition $U(0) = I$. L_l designates the Liouvillian of the radiator in the bath. We have $L_l = L_0 + l(t)$, where L_0 is the Liouvillian of the free radiator and $l(t)$ a random perturbation of the thermal bath (the plasma).

In the standard theory [1, 7], due to their great difference of mass, ions and electrons are treated in different ways, leading to:

$$L_l(t) = L_0 - \mathbf{d}\cdot\mathbf{E_l}(t) - i\Phi \tag{4}$$

where $\mathbf{E_l}(t)$ is the electric field produced by surrounding ions in a given configuration l and Φ is the electronic collisional operator. The ionic electric field is usually considered as quasi-static and is represented by its static distribution $W(E_l)$ [9]. We then have

$$I(\omega) = \Re e\frac{1}{\pi}\int_0^\infty dt e^{i\omega t}\int_0^\infty dE_l W(E_l) \ll \mathbf{d}^\dagger|e^{-iL_l t}|\mathbf{d}\gg . \tag{5}$$

If one accounts for the emitter motion, the line shape function reads:

$$I(\omega) = \Re e\frac{1}{\pi}\int_0^\infty dt e^{i\omega t} < e^{i\ \mathbf{k}\cdot\mathbf{r}(t)}\mathbf{d}(t)\cdot\mathbf{d}(0) > \tag{6}$$

with $k = 2\pi/\lambda$ and λ is the wavelength of the considered line. Broadening due to the interaction of the emitting ion with surrounding particles and that due to emitter motion are statistically dependent in the general case. Broadening due to interactions results from a modification of the internal state of the atomic oscillator. Both this internal state and the velocity of translational motion of the emitter can be altered in the same collision. In this study, interactions with the electronic component of the plasma dominate, giving rise to a phase shift of the atomic oscillator. This phase shift is due to electronic collisions which change substantially the phase without altering the velocity of the emitter owing to the great difference of masses. So, it is quite accurate to ignore correlations between the ion translation $\mathbf{r}(t)$ and the dipole moment $\mathbf{d}(t)$, and the line shape calculation involves calculation of $C(t)$ and of the self-structure factor, $S_s(k,t) =< e^{i\mathbf{k}\cdot\mathbf{r}(t)} >$, independently.

In this work, the PPP line shape code [10] is used to calculate $C(t)$. The PPP code is a multi-electron radiator line broadening code developed to calculate spectral line profiles for a general emitter in a plasma, using data for atomic energy levels and radial matrix elements generated by atomic structure codes [11]. The line profile calculations are done in the framework of the standard theory or if necessary including the effects of ionic perturber dynamics by using the Fluctuation Frequency Model [12, 13]. The self-structure factor is well known in the free-particle limit resulting from the hypothesis that each radiating ion moves at constant velocity with a Maxwellian distribution of velocities, and is given by:

$$S_s(k,t) = e^{-k^2t^2/2\beta m}, \tag{7}$$

with $\beta = 1/k_B T$ and m the ion mass. A straightforward way to take into account interactions between ions in the calculation of the line shape, is to use a classical molecular dynamics simulation techniques (MD) to compute $S_s(k,t)$. The plasma model consists of classical point ions interacting together through a coulombic potential screened by electrons and localized in a cubic box of side L with periodic boundary conditions. Newton's equations of particle motion are integrated by using a velocity-Verlet algorithm using a time-step consistent with energy conservation. Due to periodic boundary conditions, $k = 2\pi/\lambda$ must satisfy:

$$k_{x,y,z} = n_{x,y,z} 2\pi/L, \tag{8}$$

$n_{x,y,z}$ being an integer number. The number of particules, N (thus L), is chosen to find k as close as possible to that of the considered laser line. Integrating the Newton's equation gives access to the positions and velocities of the ions as a function of time and thus to the associated static and dynamic statistical properties such as structure factors, velocity correlation functions, diffusion coefficients, ion-ion collision rates, etc.

III. RESULTS

Spectral line shape calculations have been performed for the Ni-like Ag laser $4d-4p$ ($J = 0-1$) line at 13.9 nm for different densities and temperatures. The different causes of broadening (radiative decay, interaction with surrounding particles and Doppler effect) have been investigated. It has been checked that the Stark effect associated with the ion microfield has a negligible contribution to the line profile. The homogeneous broadening which consists in natural broadening and electronic collisional broadening has been calculated by using the PPP code. Accounting for both effects does not yield difficulties as they are statistically independent, giving rise to a line width equal to the sum of the respective line widths. In the following, this broadening will be referred to as lifetime broadening. The broadening due to the translational motion of the emitter (Doppler effect) has been obtained by using the self-structure factors computed by MD simulations in order to account for velocity changing effects and by Eq. 7 (free-particle limit) for comparisons. The chosen density and temperature ranges are consistent with the ones required to induce population inversions in Ni-like Ag with the collisional excitation pumping scheme. Electronic densities are in the range $5 \times 10^{19} - 8 \times 10^{20}$ cm^{-3}, the electron temperature can vary between 200 and 700 eV depending on the parameters of the pulse of the laser used to create the plasma. The ionic temperature ranges between 20 and 50 eV for transient pumping regime, and is of the order of 200 eV for QSS regime. In the following, two series of results corresponding respectively to transient ($T_i = 20$ eV, $T_e = 200$ eV) and QSS ($T_i = T_e = 200$ eV) pumping, are presented for different electronic densities.

Some typical numbers for the physical quantities of the simulated plasmas and some technical details of the MD simulations are given in Table I. In the cases of interest, the plasma coupling parameter $\Gamma = Z^2 e^2/(r_0 k T_i)$, r_0 being the ion sphere radius, $r_0 = (3/(4\pi N_i))^{1/3}$, takes values from ~ 0.6 to ~ 14. The number of particles, N, in the simulation box has been chosen equal to 300 whatever the conditions, permitting to find k satisfying Eq. 8 and kr_0^{MD} matching the laser wave number $kr_0^{\rm laser}$. The plasma frequency, $\omega_{\rm pi} = \sqrt{\dfrac{4\pi N_i (Z_i e)^2}{m}}$, and the Doppler frequency widths $\Delta\omega_D$ obtained in the free particle limit for the two pumping schemes are also given in Table I.

N_e (cm^{-3})	$\Gamma_{\rm trans}$	$\Gamma_{\rm QSS}$	N	$kr_0^{\rm laser}$	$kr_0^{\rm MD}$	$\omega_{\rm pi}$ (eV)	$\Delta\omega_{\rm D}^{\rm trans}$ (eV)	$\Delta\omega_{\rm D}^{\rm QSS}$ (eV)
5×10^{19}	5.79	0.58	300	2.03	2.016	2.57×10^{-3}	2.95×10^{-3}	9.34×10^{-3}
1×10^{20}	7.29	0.73	300	1.61	1.647	3.64×10^{-3}	–	–
2×10^{20}	9.19	0.92	300	1.28	1.302	5.14×10^{-3}	–	–
4×10^{20}	11.57	1.16	300	1.01	1.008	7.27×10^{-3}	–	–
7×10^{20}	13.95	1.39	300	0.82	0.843	9.62×10^{-3}	–	–

TABLE I. Some characteristic quantities used in MD simulations

A. Transient pumping regime

Here, the ionic temperature is relatively low ($T_i = 20$ eV) and the electronic densities are in the range $5\times10^{19} - 7\times10^{20}$ cm^{-3}. Thus, the plasma coupling parameter Γ takes values from ~ 6 to ~ 14. The corresponding plasmas are strongly coupled making the concept of binary collision between ions compromised because the ions are always in interaction with each others. Collective effects involving multiple collisions are expected to affect the profiles.

The contributions of the different broadening mechanisms to the $4d-4p$ lasing line in the case of transient regime have been calculated and the results are summarized in Fig.1.

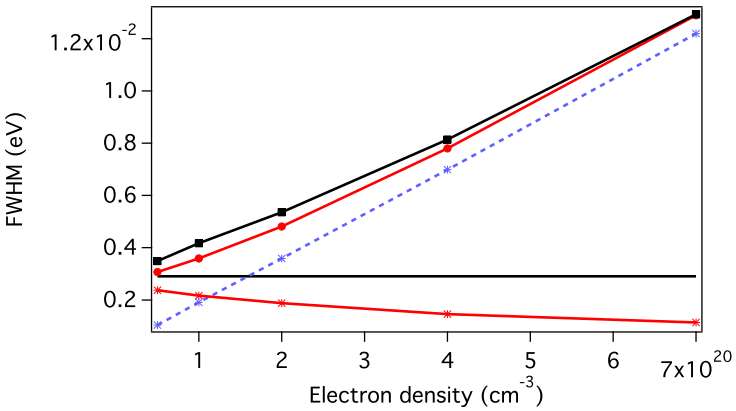

FIG. 1. (Color online) Full-width at half-maximum versus density of the $4d-4p$ laser line in the transient pumping case. Broadening due to radiator motion -in the free particle limit (Doppler broadening): black line, -accounting for particle interactions: red line and stars, lifetime broadening: blue dash line and stars. Total broadening (radiator motion + finite lifetime effects) -in the free particle limit: black line and squares, -and accounting for interactions: red line and circles.

Figure 1 shows the overall spectral linewidth (FWHM) of the $4d-4p$ laser line as a function of the electron density, as well as the individual contributions of the radiator motion and of the radiative lifetime to the broadening. Broadening due to the radiator motion has been obtained by MD simulations accounting for interactions between particles (red line and stars) and is compared to the limit of free particles (full black line) obtained by using Eq. 7. Here, the velocity-changing

narrowing is clearly seen even though when accounting for lifetime broadening (blue dash line and stars), the total profile is less altered (circles compared to squares). It can be seen that taking into account interactions between ion emitter and other ions of the plasma gives rise to a narrowing of the Doppler profile whatever the considered densities, and this narrowing increases with the density.

B. QSS pumping regime

The same study has been done for the same laser line but with $T_i = T_e = 200$ eV, i.e., for conditions that are relevant to the quasi-steady state (QSS) pumping. Four different electron densities were considered: $N_e = 1 \times 10^{20}, 2 \times 10^{20}, 4 \times 10^{20}$ and 7×10^{20} cm^{-3}. In these cases, the plasma coupling parameter falls in between 0.7 and 1.4 due to a higher ionic temperature (see table I). The line profiles have been calculated by MD simulations and the results in terms of line widths are summarized in Fig. 2.

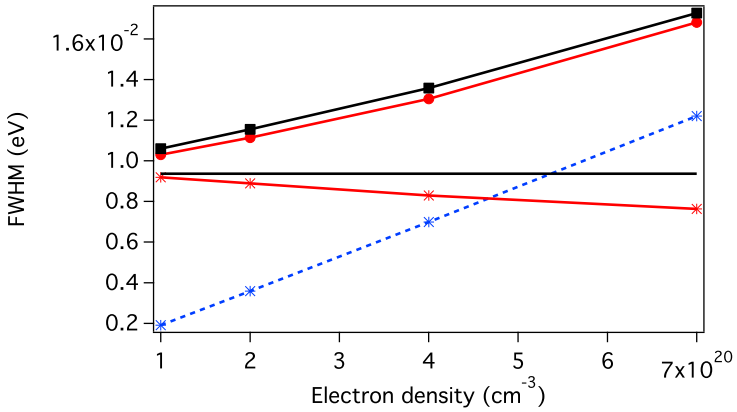

FIG. 2. (Color online) Same as Fig.1 but $T_e = T_i = 200$ eV (QSS regime).

Here again, taking into account the correlations between particles leads to a narrowing of the Doppler profile, which increases with density (or with Γ).

In both cases, the electronic collisions and spontaneous emission give rise to the lifetime broadening (blue dash line and stars) which is homogeneous and increases linearly with N_e at a given T_e. The motion of an emitting ion yields a Doppler shift of the X-ray laser line. If we assume that each radiating ion moves at constant velocity with a Maxwellian distribution of velocities, the line profile is inhomogeneous and shows a Gaussian shape with a width (full black line) given by a simple analytical formula depending only on T_i. Accounting for both of the previous effects, the resulting spectral profile will be the convolution of the homogeneous and inhomogeneous profile, leading to the so-called Voigt profile with a width which is a complex combination of both homogeneous and inhomogeneous linewidths (black line and squares). Taking into account interactions between ion emitter and other ions of the plasma gives rise to a narrowing of the Doppler profile (red line and stars) whatever the considered densities and this narrowing increases with the density. The line profile is no longer Gaussian, so the overall profile is no longer a Voigt profile. Moreover if the velocity-changing rates are large enough, the velocity redistribution can give rise to

a homogenization of the otherwise inhomogeneous profile. We will come back on this in the next section.

IV. DISCUSSION

In the following discussion, we will focus our attention on the Doppler effect and all the presented spectral lineshapes will not account for lifetime broadening.

The narrowing of the Doppler profile, observed for the two regimes of collisional excitation pumping, can be understood in terms of the correlation function $S_s(k,t)$ for a moving emitter. In the free particle limit, $S_s(k,t) = e^{-k^2t^2/2\beta m} \equiv e^{-k^2t^2\overline{v}^2/4}$, the characteristic Doppler correlation time is $\tau_D \approx \lambda/\overline{v}$. τ_D can then be seen as the time taken by a radiator having the mean thermal velocity $\overline{v}$ to move a distance equal to the laser emission line λ. Any factor restricting or hindering the movement of the emitter will broaden $S_s(k,t)$ and hence narrow the line shape. Due to the strong coupling plasma parameters involved here, ions are in constant interaction and they are more and more hindered to move freely as the density increases.

For a better understanding, profiles obtained for different densities have been plotted on the same graph in logarithmic units. Due to the different Doppler widths, the two sets of results

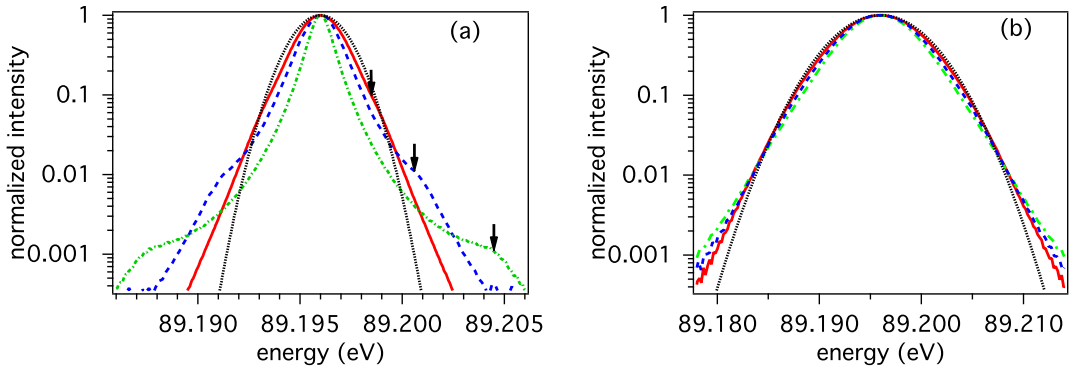

FIG. 3. (Color online) Spectral $4d-4p$ line Doppler profiles accounting for ion correlations in the case of the transient pumping regime, $T_i = 20$ eV, (a) and of the QSS pumping regime, $T_i = 200$ eV, (b). Red full line: $N_e = 5\times10^{19}$ cm^{-3} (a) and $N_e = 1\times10^{20}$cm^{-3} (b), blue dash line: 2×10^{20} cm^{-3}, and green dash-dot line: 7×10^{20} cm^{-3} . The black dot curve corresponds to the Doppler profile in the free particle limit and the arrows mark the position of oscillation frequency of the velocity autocorrelation function.

obtained for the two regimes of collisional pumping have been plotted on two different graphs, fig.3(a) for $T_i = 20$ eV and fig.3(b) for $T_i = 200$ eV. It can be noticed that the profiles present different features. When one accounts for ionic correlations, the line profiles, in the case of transient pumping are not only narrowed but a shoulder structure appears in the wings more or less far from the center depending on the density. While in the cases of QSS pumping, the line shape is modified and the width reduced but no structures are apparent in the wings. The frequency shifts, $\Delta\omega_{\rm osc}$, delimiting the position of the shoulders are shown by black arrows in Fig.3(a). We have checked that the values of those frequency shifts are actually close to the ionic plasma frequency for the

given N_e, and they correspond to the frequencies of oscillations of the velocity autocorrelation functions, $C_v(t) =< \mathbf{v}(t) \cdot \mathbf{v}(0) >$ which reveals the properties of single-particle motion in the plasma. $C_v(t)$ is obtained by MD simulations and the oscillation frequencies, $\Delta\omega_{\rm osc}$ are deduced from $C_v(t)$ by Fourier transform. Examples of velocity autocorrelation functions and their Fourier transforms are given in Fig.4(a) and Fig.4(b), respectively for different values of Γ. The decay of $C_v(t)$ is characterized by the appearance at large times of oscillations at a frequency close to $\omega_{\rm pi}$. The oscillations are already seen at $\Gamma = 5.786$ ($N_e = 5 \times 10^{19}$ cm^{-3}) and become more pronounced as Γ increases. They are due to the coupling between the collective density fluctuations and the single particle motion [14].

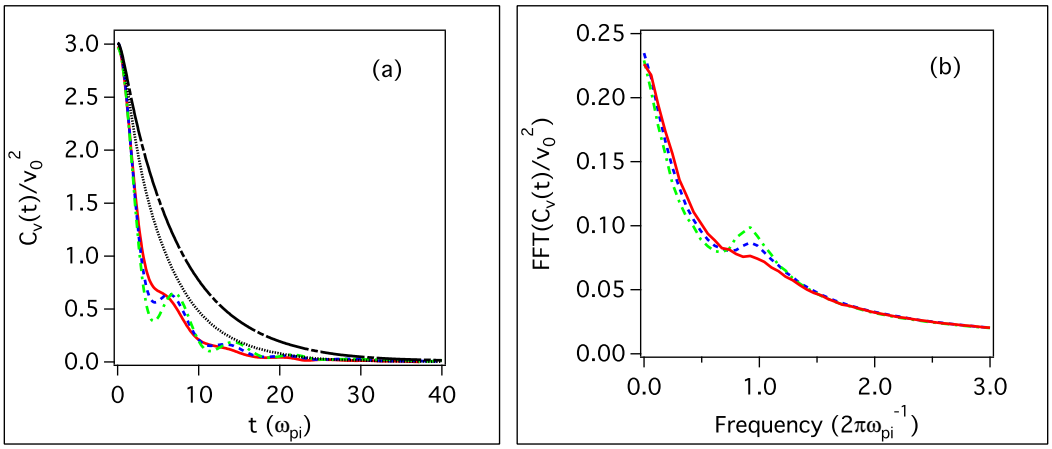

FIG. 4. (Color online) Velocity autocorrelation function (a) for a nickel-like silver plasma. Short dash-dot black line: $\Gamma = 0.73$, dot black line: $\Gamma = 1.39$, full red line: $\Gamma = 5.79$, dash blue line: $\Gamma = 9.19$, dash-dot green line: $\Gamma = 13.95$. The Fourier transforms for Γ=5.79, 9.19 and 13.95 are plotted on graph (b). The velocities are in units of $\sqrt{kT_i/m}$ and the time in units of $\omega_{\rm pi}^{-1}$.

In order to have a better understanding of the dynamics of a particle in those plasmas, the evolution in time of the frequency distribution associated to the set of particles chosen to have an initial velocity $\mathbf{v}(0)$ such as $\mathbf{k}\cdot\mathbf{v}(0) = \omega \pm \Delta\omega$ have been plotted on Fig.5 for $\omega = 0$ and a $\Delta\omega$ chosen sufficiently large to have a representative number of tagged particles. The plasma conditions are those of the QSS pumping regime at $N_e = 1 \times 10^{20}$ cm^{-3}. The sharper distribution corresponds to the initial time for which the particles such as $\mathbf{k} \cdot \mathbf{v}(0) = 0$ will emit at a frequency equals to $\omega_0 \pm \Delta\omega$ and as the time increases the frequency distributions become broader and broader and tend to the infinite limit time corresponding to the frequency distribution given by the equilibrium velocity distribution, i.e., the Doppler distribution in the free particle limit (black dash curve). Four different times of evolution (0.24 ω_{pi}^{-1}, ω_{pi}^{-1}, 2.5 ω_{pi}^{-1} and 3.83 ω_{pi}^{-1}) have been chosen, the last one corresponding to the radiative lifetimes. It can be seen that during their effective lifetimes, the radiating and absorbing ions sample many velocities, not just one as it is supposed in the Doppler free particle limit. The effect of this velocity redistribution will be to homogenize the Doppler component of the intrinsic line profile. Similar results have been obtained in the transient pumping regime. Another important effect which can be seen in this figure is that interactions between particles give rise to small changes in the velocity at short time-scale: the frequency

redistribution at $t = 0.24\ \omega_{\rm pi}^{-1}$ is limited to frequencies around the initial frequencies suggesting that the interactions give rise to small-angle scattering. Moreover, it is necessary to wait long enough to fill the entire distribution. This behavior suggests that the dynamics of the ions in those plasmas could be modeled by a Brownian-movement model [5, 15].

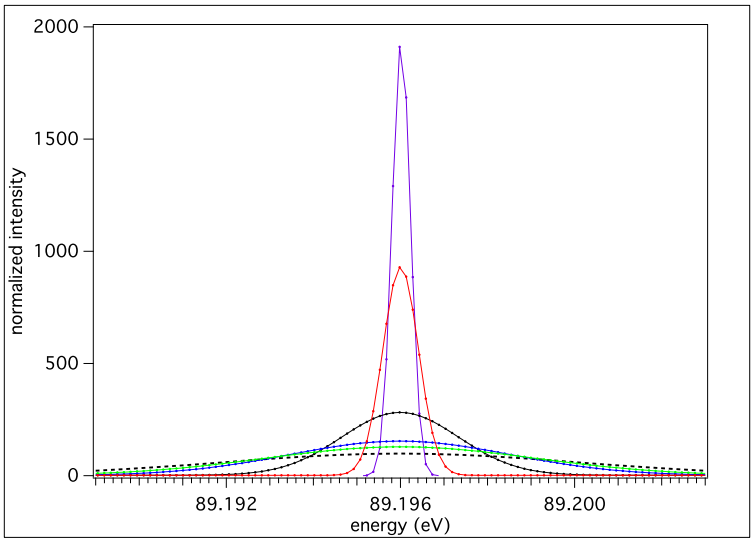

FIG. 5. (Color online) Evolution in time of the frequency distribution function of particles with an initial velocity such as $\mathbf{k}\cdot\mathbf{v}(0) = 0 \pm \Delta\omega$ for conditions of the QSS regime at $N_e = 1\times10^{20}$ cm^{-3} and for $t = 0$ (purple), 0.24 $\omega_{\rm pi}^{-1}$ (red), ω_{pi}^{-1} (black), 2.5 ω_{pi}^{-1} (blue) and 3.83 ω_{pi}^{-1} (green), from the highest to the lowest curve respectively. The black dash line corresponds to the Doppler free particle limit that would be reached at infinite time.

In this model, the following expression was derived for the self-structure factor:

$$S_s(k,t) = e^{-\frac{k^2}{2}<x_k^2>}, < x_k^2 >= \frac{\bar{v}^2}{\nu_d^2}(\nu_d t - 1 - e^{-\nu_d t}) \tag{9}$$

where $< x_k^2 >$ is the mean square displacement in the direction of k over the time t and $\bar{v} = \sqrt{2k_B T_i/m}$. It is shown in [15] that ν_d is related to $C_v(t)$ by:

$$C_v(t) \equiv < \mathbf{v}(t)\cdot\mathbf{v}(0) >= \frac{3}{2}\bar{v}e^{-\nu_d t}. \tag{10}$$

The values of ν_d have been obtained by fitting with an exponential function the velocity autocorrelation functions obtained by MD simulations. These values have been used in Eq. 9 to obtain $S_s(k,t)$ and the frequency distribution has been derived from $S_s(k,t)$ by Fourier transform. The results are presented in Fig.6. The Brownian-movement model gives a good approximation of the frequency distribution in the two considered regimes of collisional excitation whatever the densities, even though the wings and the shoulder structures are not reproduced correctly. This is due to the fact that, as it can be seen on Fig.4, the velocity autocorrelation function, $C_v(t)$, can be very far from an exponential function. Fitting $C_v(t)$ by an exponential form has not only the disadvantage

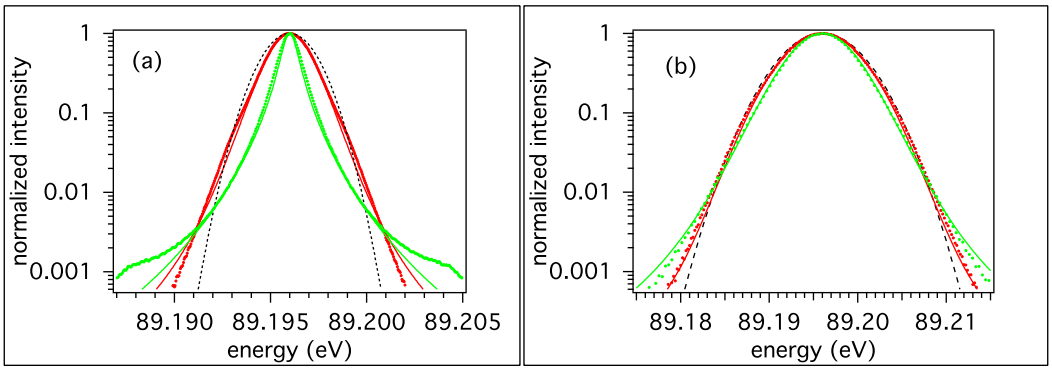

FIG. 6. (Color online) Comparisons of the spectral $4d-4p$ line profiles in the case of the transient pumping for $N_e = 5\times10^{19}$ (green) and $N_e = 7\times10^{20}$ (red) (a) and of the QSS pumping for $N_e = 1\times10^{20}$ (green) and $N_e = 7\times10^{20}$ (red) (b). The dots represent the MD simulation results, the full line the Brownian-movement model results and the black dot curve corresponds to the Doppler profile in the free particle limit.

of eliminating the oscillations expected at a frequency near $\omega_{\rm pi}$ but also in the plasmas of interest here, where the diffusing particles are similar to their neighbors, the Markovian approximation used in the Brownian-movement model which ignores any memory associated with the motion of the particle is not valid [15]. Nevertheless, in order to propose a rapid way to model the intrinsic line profile necessary in radiative transfer calculations, the Brownian-movement model without memory gives a good approximation in the conditions consistent with the two XUV laser regimes, transient and QSS.

V. CONCLUSION

This paper concerns a study of the effects of particle correlations on the line broadening due to the radiator motion in the particular case of XUV laser lines. Two kinds of laser have been considered, transient XUV laser for which ionic temperature is relatively low, so the plasma coupling parameters is large, and quasi steady state XUV laser for which the ionic temperature is higher and the plasma coupling parameter of the order of 1. It has been shown that the effect of correlations cannot be neglected in evaluating Doppler effect for the cases of interest. The numerical simulation gives the right answer to the problem of the intrinsic spectral line shape but it is not well adapted to a line transfer calculation. It has been shown that the Brownian-movement model applied to the calculation of the self-structure factor gives a good approximation of the Doppler spectral line shape provided the velocity autocorrelation function is known. Another result concerns the velocity redistribution which homogenizes the Doppler component of the intrinsic profile. The future work will be to investigate how the results obtained in this paper will influence the behaviour of the spectral profile when it is amplified in the plasma. In medium with gain, the observed profile is modified by radiative transport effects and these modifications depend on the homogeneous or inhomogeneous nature of the intrinsic profile. In general, the line profile is described by a Voigt profile which is the convolution of the Lorentzian profile due to finite lifetime and the Gaussian profile due to Doppler effect (due to the radiator motion). It has been shown in this paper that for

all the considered densities and temperatures, the radiator-motion broadened profiles are modified by taking into account correlations between particles, being homogenized by velocity redistribution whatever the conditions and narrowed essentially in the transient regime.

---

[1] H.R. Griem, *Spectral line broadening by plasmas*, (Academic, New York, 1974).
[2] H.R. Griem, Phys. rev. A **33**, 3580 (1986).
[3] E.L. Pollock and R. A. London, Phys. Fluids B **5**, 4495 (1993).
[4] J.A. Koch et al., Phys. Rev. A **50**, 1877 (1994).
[5] S.G. Rautian and I.I Sobel'man, Usp. Fiz. Nauk **90**, 209 (1966).
[6] G. J. Pert, JOSA B **11**, 1425 (1994).
[7] H.R. Griem, *Principles of Plasma Spectroscopy*, (Cambridge University Press, 1997).
[8] R.H. Dicke, Phys. Rev. **89**, 472 (1953).
[9] C.A. Iglesias et al., Phys. Rev. A **31**, 1698 (1985); C.A. Iglesias, et al., J. Quant. Spectrosc. Radiat. Transf. **65**, 303 (2000).
[10] A. Calisti et al., Phys. Rev A **42**, 5433 (1990).
[11] I.P. Grant et al., Comput. Phys. Commun. **21**, 207 (1980).
[12] B. Talin, A. Calisti, L. Godbert, R. Stamm, R.W. Lee and L. Klein, Phys. Rev. A **51**, 1918 (1995).
[13] A. Calisti et al., Phys Rev. E **81**, 016406 (2010).
[14] J.P. Hansen, I. R McDonald and E.L. Pollock, Phys. Rev. A **11**, 1025 (1975).
[15] J.P. Hansen and I. R McDonald, *Theory of Simple Liquids*, (Academic Press, London, 1976).